Int J Clin Exp Pathol 2017;10(3):3677-3690
www.ijcep.com /ISSN:1936-2625/IJCEP0046859

Original Article

High-resolution array based heterogeneity and clonality profiling of oral squamous cell carcinoma: genetic relationship between metastatic primary tumor and the paired lymph node metastases

Bing Wen[1], Fang-Ling Zhang[2], Wei Yang[3], Wen-Wei Zhou[4], You-Chun Wei[1], Sheng-Chang Deng[2], Na Li[1], Yan-Xi Huang[1], Xue-Jiao Cheng[1]

[1]Department of Stomatology, The First Affiliated Hospital of Nanchang University, Nanchang, China; [2]College of Pharmacy, Nanchang University School of Medicine, Nanchang, China; [3]Department of Stomatology, Jiangxi Provincial Tumor Hospital, Nanchang, China; [4]Department of Oral and Maxillofacial Surgery, Jiujiang University Hospital, Jiujiang, China

Received September 23, 2016; Accepted December 27, 2016; Epub March 1, 2017; Published March 15, 2017

Abstract: We investigated heterogeneity and clonality based genetic relationships between primary tumors of oral squamous cell carcinoma (primary) and metastases utilizing the high-resolution array based comparative genomic hybridization approach. Total 50 tumor samples (from 30 metastatic primary tumors patients) were collected and subjected to comparative genomic hybridization (a high-resolution array). Genetic profiles of these tumors were compared with their paired lymph node metastases while the genetic profiles of non-metastatic primary tumors were compared with lymph node metastases. Distinctive differences were found in the patterns of genomic profiles of metastatic primary tumors and their paired lymph node metastases. Paired samples had higher similarity scores than non-paired samples. Minor populations with different copy number aberrations were also found in metastatic oral squamous cell carcinoma. Further copy number aberrations were compared between grouped samples of lymph node metastases and metastatic primary tumors to identify copy number aberrations with respect to lymph node metastasis. We concluded that genetically clonal tumor cells are predominantly responsible for the composition of metastatic primary tumors and their paired lymph node metastases and minor populations with different copy number aberrations may also exist in metastatic oral squamous cell carcinoma.

Keywords: Heterogeneity, clonality, oral squamous cell carcinoma, comparative genomic hybridization, copy number aberration

Introduction

Head and neck cancer is found to be in the sixth place of existence of most common human cancer in the world [1]. Among them almost half of these cases are located in the oral cavity. Except less than 10% cases all are oral squamous cell carcinoma (OSCC) cases [2]. Each year 0.3 million new cases of OSCC are being diagnosed [3]. Each year, more than 10 thousand new cases in Japan [4], 40 thousand new cases in the EU and 35 thousand new cases in the US [2] are being recorded. The association of half decrease in the half decade patients' survival with OSCC is related with the presence of cervical lymph node metastasis [5, 6]. That's why it is very important to predict or detect the presence of lymph node metastasis for the sake of effective treatment of OSCC. As per several reports the imaging techniques such as ultrasonography, CT and MRI are not beyond question of reliability for detection of micrometastases due to high incidence of occult neck disease in these cases [7-12]. So far, many parameters such as altered gene expression, thickness and size of primary tumors found useful for the identification of high-risked occult node metastasis in node-negative patients [13-16] even then the mechanism of spreading of tumor cells is not still clear [17]. Initially, studies of the development and progression of colorectal and pancreatic cancers revealed a concept called as the "multi-

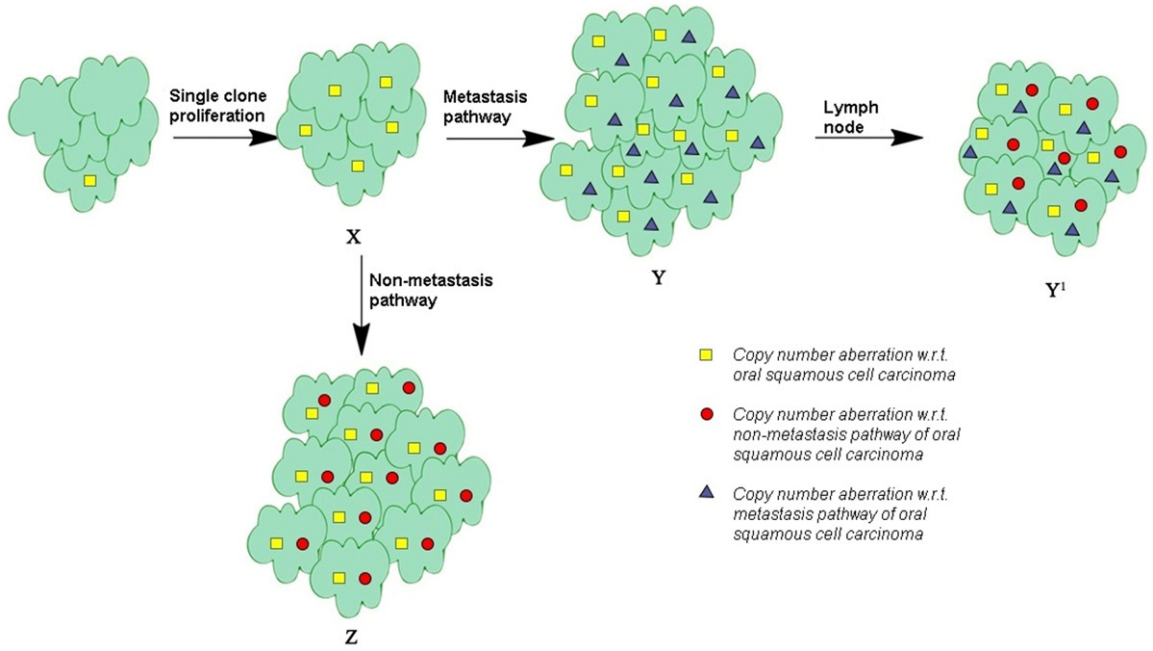

Figure 1. In our proposed model for the development of metastasis and non-metastasis pathways for OSCC; it originates from single cell (shown in green colored structure) containing one genomic aberration (shown in small yellow box). This single clone then proliferates to change into X. During this process some tumor cells randomly acquire additional mutations and hence forms a forms a unique subpopulation in the primary tumor in either of the metastasis (Y) and non-metastasis pathways (Z). Through clonal evolution some of the metastasis can spread to cervical lymph nodes (Y').

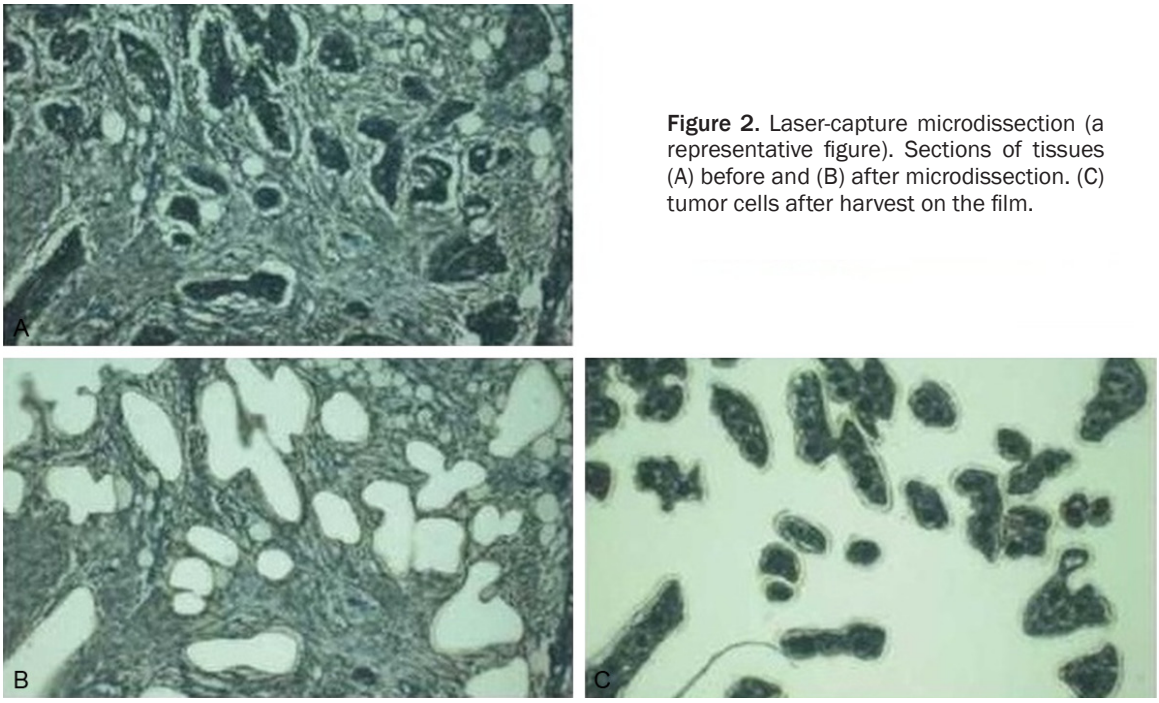

Figure 2. Laser-capture microdissection (a representative figure). Sections of tissues (A) before and (B) after microdissection. (C) tumor cells after harvest on the film.

step tumorigenesis model" which had referred the accumulation of chromosomal aberrations [18].

Recently, the "clonal evolution model" has been established as an extension of previous model and in this new model a single clone is

Table 1. Clinicopathological characteristics of the patients subjected in our study

	Sample ID (Sex) M = male; F = Female	Age	Site	Stage	Histological differentiation	Metastatic neck lymph node	Delayed lymph node metastasis	Primary tumor thickness (mm)
Source tissue: Oral squamous cancer cell metastatic primary tumor	Case 1 (M)	47	Tongue	T2N2bM0	Well	+	-	11
	Case 2 (M)	67	Floor of mouth	T2N2cM0	Well	+	-	2
	Case 3 (F)	70	Tongue	T2N0M0	Well	+	+	6
	Case 4 (F)	68	Gingiva	T3N0M0	Moderate	+	+	4
	Case 5 (F)	77	Tongue	T2N0M0	Well	+	+	4
	Case 6 (F)	88	Gingiva	T2N0M0	Well	+	+	10
	Case 7 (F)	76	Tongue	T1N0M0	Well	+	+	3
	Case 8 (F)	78	Tongue	T2N0M0	Well	+	+	5
	Case 9 (M)	62	Tongue	T2N0M0	Well	+	+	7
	Case 10 (M)	69	Tongue	T2N0M0	Well	+	+	8
	Case 11 (M)	57	Floor of mouth	T2N2cM0	Well	+	+	4
	Case 12 (F)	73	Tongue	T2N0M0	Well	+	+	5
	Case 13 (M)	71	Buccal mucosa	T2N0M0	Well	+	+	6
	Case 14 (F)	73	Buccal mucosa	T1N0M0	Well	+	+	11
	Case 15 (M)	75	Floor of mouth	T1N0M0	Moderate	+	+	2
	Case 16 (F)	69	Buccal mucosa	T4N0M0	Well	+	+	2
	Case 17 (M)	64	Tongue	T2NM0	Well	+	+	7
	Case 18 (M)	58	Tongue	T1N0M0	Well	+	+	7
Source tissue: Oral squamous cancer cell neck lymph-node metastasis	Case 1 (M)	47	Tongue	T2N2bM0	Well	+	+	11
	Case 2 (M)	67	Floor of mouth	T2N2cM0	Well	+	+	2
	Case 3 (F)	70	Tongue	T2N0M0	Well	+	+	6
	Case 4 (F)	68	Gingiva	T3N0M0	Moderate	+	+	4
	Case 5 (F)	77	Tongue	T2N0M0	Well	+	+	4
	Case 6 (F)	88	Gingiva	T2N0M0	Well	+	+	10
	Case 7 (F)	76	Tongue	T1N0M0	Well	+	+	3
	Case 8 (F)	78	Tongue	T2N0M0	Well	+	+	5
	Case 9 (M)	62	Tongue	T2N0M0	Well	+	+	7
	Case 10 (M)	69	Tongue	T2N0M0	Well	+	+	8
	Case 11 (M)	57	Floor of mouth	T2N2cM0	Well	+	+	4
	Case 12 (F)	73	Tongue	T2N0M0	Well	+	+	5
	Case 13 (M)	71	Buccal mucosa	T2N0M0	Well	+	+	6
	Case 14 (F)	73	Buccal mucosa	T1N0M0	Well	+	+	11
	Case 15 (M)	75	Floor of mouth	T1N0M0	Moderate	+	+	2
	Case 16 (F)	69	Buccal mucosa	T4N0M0	Well	+	+	2
	Case 17 (M)	64	Tongue	T2NM0	Well	+	+	7
	Case 18 (M)	58	Tongue	T1N0M0	Well	+	+	7
Source tissue: Oral squamous cancer cell non-metastatic primary tumor	Case 19 (F)	77	Tongue	T1N0M0	Well	-	-	4
	Case 20 (M)	59	Tongue	T3N0M0	Well	-	-	10
	Case 21 (M)	45	Tongue	T2N0M0	Well	-	-	11
	Case 22 (M)	72	Tongue	T2N0M0	Well	-	-	5
	Case 23 (F)	74	Tongue	T1N0M0	Well	-	-	4
	Case 24 (F)	84	Floor of mouth	T2N0M0	Moderate	-	-	8
	Case 25 (M)	75	Tongue	T2N0M0	Well	-	-	10
	Case 26 (M)	81	Floor of mouth	T2N0M0	Well	-	-	6
	Case 27 (F)	87	Tongue	T1N0M0	Well	-	-	5
	Case 28 (M)	76	Tongue	T1N0M0	Well	-	-	4
	Case 29 (M)	79	Tongue	T2N0M0	Well	-	-	8
	Case 30 (M)	81	Tongue	T2N0M0	Well	-	-	7

Neck lymph-node metastasis	Case 10 Lymph-node metastasis-1 (M)	69	Tongue	T2N0M0	Well	+	+	8
	Case 10 Lymph-node metastasis-2 (M)	69	Tongue	T2N0M0	Well	+	+	8

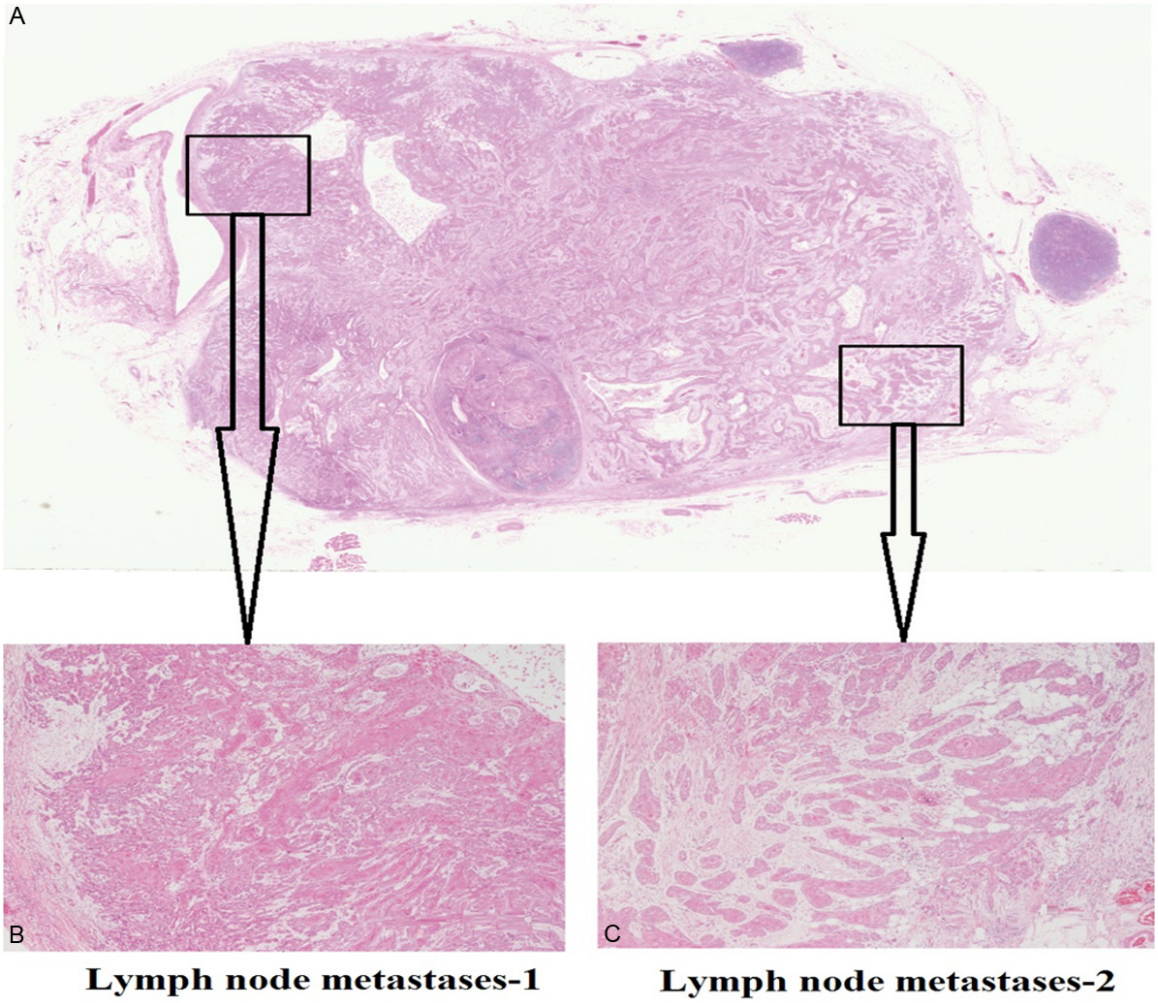

Figure 3. Genomic profiles of lymph node metastasis tissue from case 10. In (A) low- and (B and C) high-power views (after staining) (a representative figure). Laser-capture microdissection was used to collect the tumor cells in the area of (B) lymph node metastases-1 and (C) lymph node metastases-2 which was then subjected to array based comparative genomic hybridization analysis.

held responsible for several distinct subpopulations [19-21]. In these cases there is replacement of distinct subpopulations with the predominant population through the stage of tumor progression within a single tumor mass. Thus several genetically heterogeneous subpopulations were coexisted within a single tumor mass due to the effects of environmental selection pressure. These tumor progression models have their limitations and could not explain the cellular and molecular mechanisms for lymph node metastasis [22, 23]. Since genomic copy number aberrations contribute to the malignant feature of tumor cells, a comparative study of genomic profiles of a primary tumor along with their corresponding metastases should provide mechanism of the process and progress of metastasis [24].

Interestingly, an array-based comparative genomic hybridization informed us about genomic copy number aberrations [25] across the entire

genome. This kind of array identifies tumor-suppressive genes which are located in comparative genomic hybridization and thus identify regions of tumor-suppressive or oncogenic genes in OSCC [26-30]. However, relevance of copy number aberrations in lymph node metastasis' process and progress is still not explored fully. Only one study has been reported, so far, for comparing the genomic profiles of the primary tumor along with metastases utilizing comparative genomic hybridization in OSCC [28]. However, that study was limited to only eight cases and even then there was lack of comparison of the clonality of genomic profiles of the primary with their corresponding metastases. Besides, a few studies which have analyzed this relationship in head and neck squamous cell carcinoma [31, 32] have their own limitations as they used conventional metaphase comparative genomic hybridization of restricted resolution, led to incomplete characterization of genomic regions.

In the background of "punctuated clonal evolution" model [33] which is limited to small number of samples, we hypothesized a new model (**Figure 1**) for the development of metastatic OSCC in which we proposed the composition of metastatic primary tumor as genetically heterogeneous subpopulations. So far, single-cell sequencing based upon deep sequencing has never been used for the investigation of the clonal evolution of OSCC by deep sequencing. Thus we aimed herein the investigation of relationships, specifically based on gene, of OSCC's primary tumors with their corresponding metastases followed by the identification of the relation of copy number aberrations and lymph node metastasis. Hence, a high-resolution array-based comparative genomic hybridization analysis has been performed in the present study for the genomic profiling of metastatic primary tumors, their paired cervical lymph node metastases, and non-metastatic primary tumors after collecting their tumor samples followed by their comparative study.

Materials and methods

Specimen source, tissue array and genomic DNA extraction

The study was approved by the ethics review board of the First Affiliated Hospital of Nanchang University and all samples were collected from this hospital and written consent was obtained from all the patients. The study patients were selected and their medical records analyzed retrospectively. Thirty patients having scattered tumors without multiple occurrence were chosen and subjected to surgical OSCC tumors resection in our hospital. First tissues were fixed by formalin and then embedded with paraffin before their sections were cut and subjected to histological analysis through staining using hematoxylin-eosin and with toluidine blue (Beijing, China) for extraction purpose of genomic DNA (**Figure 2**). As shown in **Table 1**, we collected 50 samples (from 30 patients). These 50 samples include 18 paired samples of metastatic primary tumors and their corresponding lymph node metastases, 12 samples of non-metastatic primary tumors, as well as 2 samples of lymph node metastases from case 10 (**Figure 3**) by using laser-capture microdissection (ArcturusXT, Beijing, China).

We focused on random selection of patients with metastatic OSCCs; even then, we selected non-metastatic OSCCs with a tumor thickness of more than 4 mm, so that any selection bias in terms of tumor thickness could be reduced. Hence we could not find statistically significant value of the difference of median (P=0.591, using Mann-Whitney U test) tumor thickness between metastatic primary tumors and non-metastatic primary tumors. Proteinase K digestion method was used for genomic DNA extraction which was further followed by extraction using phenol and chloroform. Genomic DNA was also extracted, separately as the source of control DNA from normal renal cortex of 15 patients with renal or ureteral pelvic carcinoma.

High-resolution array based comparative genomic hybridization

Precisely, 44 k oligonucleotide comparative genomic hybridization arrays (Agilent Technologies, Beijing, China) were used for the analysis. The manufacturer's protocol was used for labeling and hybridization. For this purpose, AluI and RsaI (Promega, Beijing, China) were used for the digestion of 1.8-2.2 μg of tumor DNA. For control we took an equal amount of control DNA. After digestion, Cy5-dUTP and Cy3-dUTP were used to label the tumor and control DNAs, respectively, through Genomic DNA Labeling Kit Plus (Agilent Technologies), which were further subjected to Microcon YM-30 filters (Millipore, Beijing, China), and then whole sample was concentrated to 81.8 μl. These were then pooled so that they could be mixed with human Cot-1 DNA before dissolv-

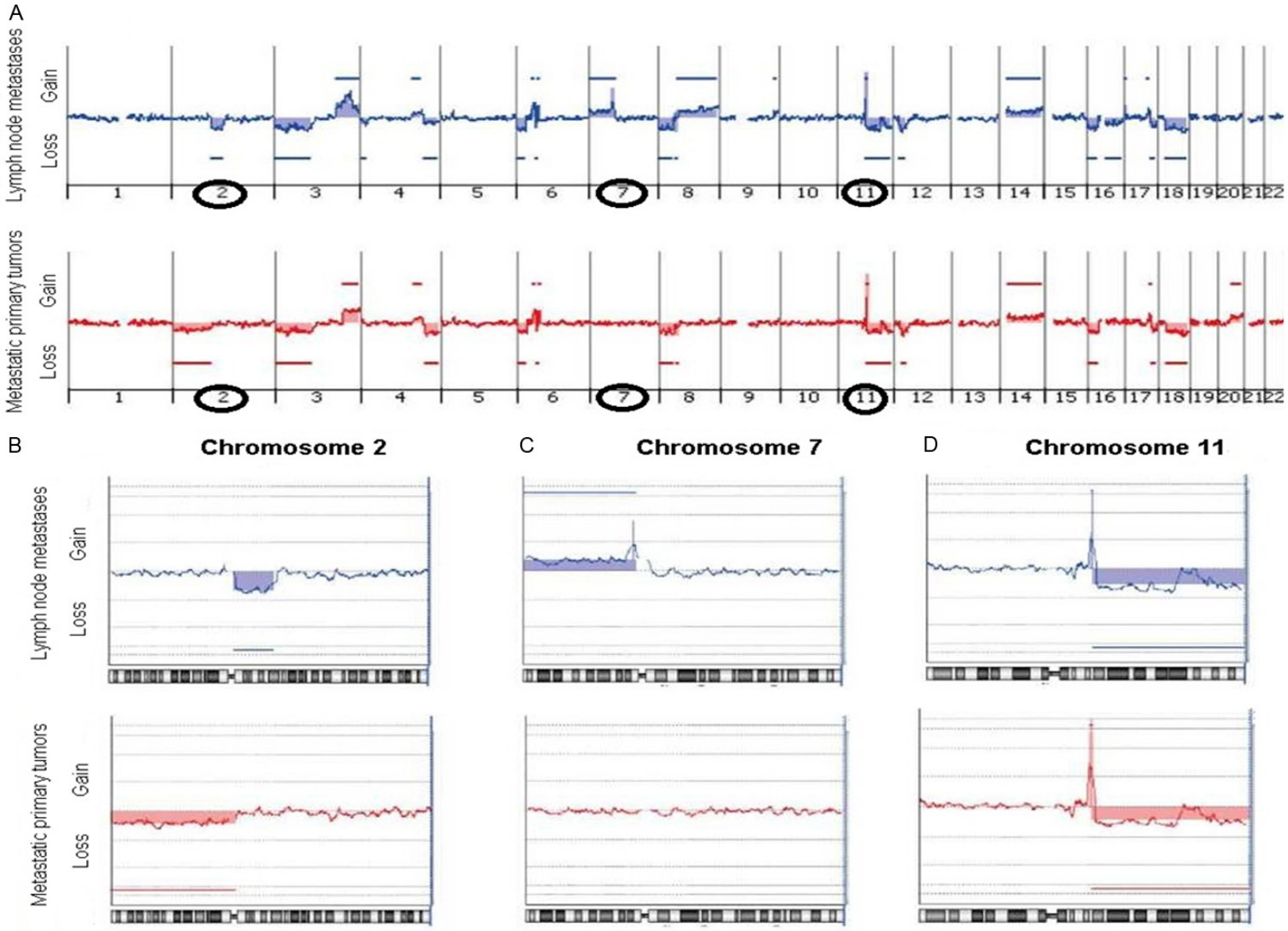

Figure 4. Genomic profile of a metastatic primary tumor and the corresponding paired lymph node metastases of a metastatic OSCC (a representative figure). (A) Paired samples of lymph node metastases (above) and metastatic primary tumor (below) from case 10. Detailed genomic profiles of Chr2, Chr7 and Chr11 encircled are respectively shown in (B-D).

ing in hybridization buffer. Then the samples were further denatured and hybridized to the comparative genomic hybridization array at 70°C for 24 h. As per manufacturer's protocol glass slides were scanned after washing.

Data analysis

Feature Extraction (v.9.5.3.1; Agilent Technologies) with linear normalization was utilized for the analysis of microarray images. DNA Analytics (v.4.0.8.1; Agilent Technologies) was used to import the resulting data. The log2 ratio values of Cy5 (tumor) to Cy3 (control) was calculated after normalizing the raw data. At a threshold of 7.0 the ADM-2 algorithm was used to determine the aberrant regions. The aberration filter parameters were chosen as: minimum number of probes in region 2, percentage penetrance per feature 0, minimum absolute average log2 ratio for region 0.171 and maximum number of aberrant regions 10 k were set for detecting gains and losses. In order to confirm this we set reference CGH vs reference analyses on same the aberration filters (using the ADM-2 algorithm) and detected no aberrant region (data not shown). Hence we confirmed the sufficiently conservative nature of our parameter setting as it yielded nearly zero false positivity rates. The X and Y choromosomes mapped probes data were eliminated. The qualities of array and all copy number aberrations detected in each sample data were also summarized (data not shown). Further, concordance rates between paired or non-paired metastatic primary tumors and lymph node metastases were also calculated. The cluster merge option along with correlation were chosen with respect to complete shrinkage as the similarity metric in unsupervised hierarchical clustering (as default settings of Gene cluster software (version 3.0)). Fisher's exact test and paired t-test were used for statistical calculations, considering the differences at $P<0.05$ as statistically significant values.

Results

Genetic relationship between metastatic primary tumor and the paired lymph node metastases in metastatic OSCCs

We analyzed the genomic profiles of 18 pairs of metastatic primary tumor and lymph node metastases pairs using array-based comparative genomic hybridization, for this purpose. Case 10 was shown in **Figure 4** as our representative case. Across the entire genome a similar profile pattern was shared between the metastatic primary tumor and paired lymph node metastases of this case (**Figure 4A**). However, in some cases (2q, 2p, 7p and 16q) we found distinct genomic aberrations (**Figure 4A**). In the lymph node metastases (but not in the metastatic primary tumor) the loss of 2q and gain of 7p were observed while loss of 2p was observed in the metastatic primary tumor (but not in the lymph node metastases) (**Figure 4B** and **4C**). Specifically, results in chromosome 11q supported the clonal relation between the tumor cells in the metastatic primary tumor and paired lymph node metastases of this case (**Figure 4D**). These results have suggested that in this case the genetically distinct subpopulations have composed metastatic primary tumor and paired lymph node metastases. Separate dissection on tissue sections of lymph node metastases from case 10 was performed so that we can get the geographical distribution of subclones. Tumor cells from two sites on the lymph node metastases tissue sections were collected and genomic aberrations were analyzed by using array based comparative genomic hybridization procedure (**Figure 3A-C**). In this case 10, differences in the log2 ratio of aberrations were found but couldn't clarify the difference observed between genomic aberration patterns (data not shown). We also found slightly higher intensity of 11q13 amplification in lymph node metastases-1 than in lymph node metastases-2. Similarly, higher intensity of 7p-12 amplification was observed in lymph node metastases-2 than in lymph node metastases-1 (detailed data not shown) and hence we found the clonal composition of these two sites with genetically distinct subclones. On the other hand similarity of the aberration pattern of chromosome 3q of lymph node metastases-1 more to that of metastatic primary tumor than to that of lymph node metastases-2 has led us to the conclusion that tumor cells in lymph node metastases-1 might have more close relation with those in metastatic primary tumor (detailed data not shown).

Besides case 10, the genomic profiles of rest 17 paired metastatic primary tumor and lymph node metastases samples were also compared individually and found similar patterns of copy

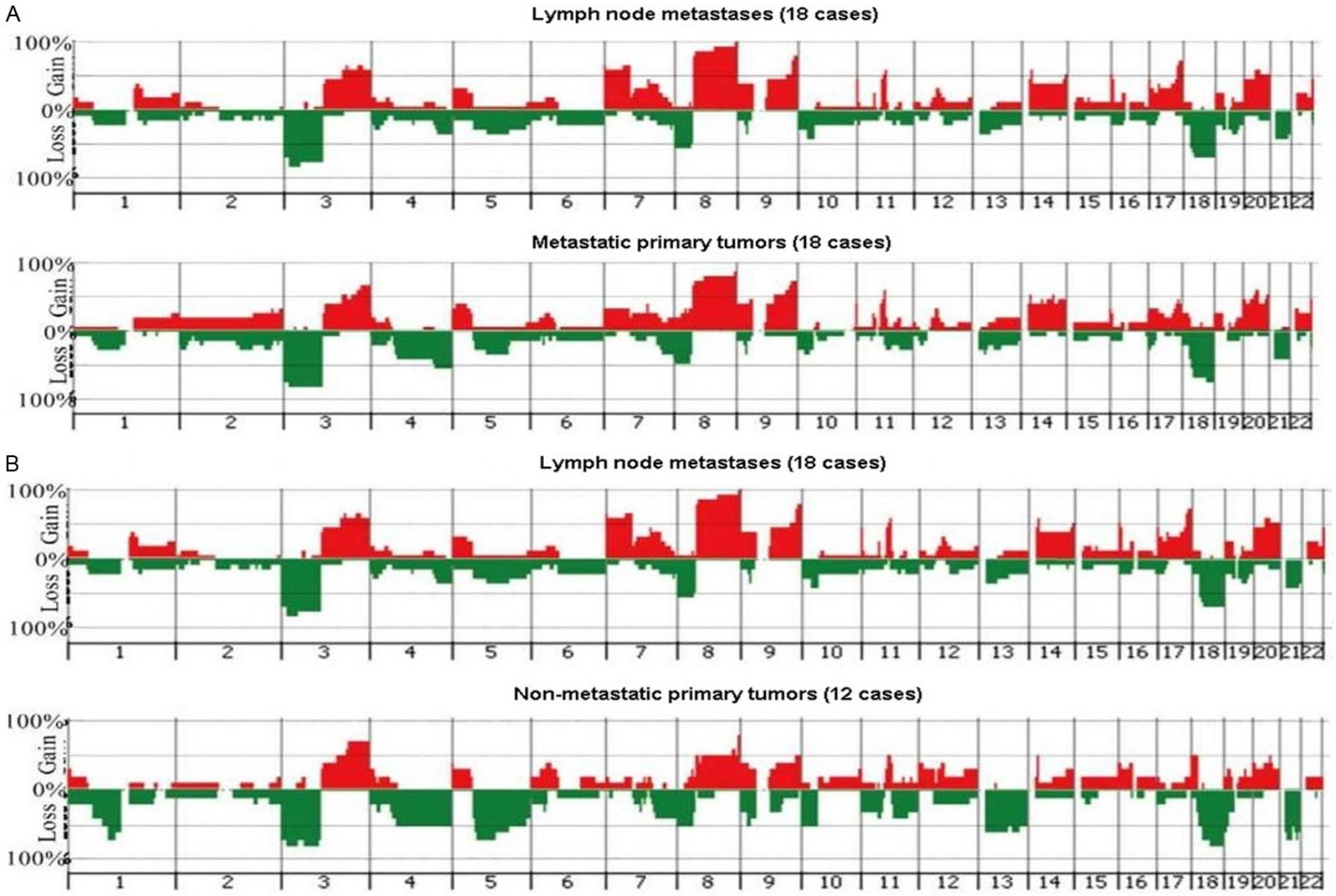

Figure 5. Genomic profile frequencies of copy number aberrations in (A) the metastatic primary tumors and corresponding paired of lymph node metastases in the 18 cases, (B) the 18 lymph node metastases and 12 non-metastatic primary tumors. Frequency (%) of gains (positive axis) and losses (negative axis) are shown on vertical lines for each probe. Oligonucleotide probes are shown on horizontal lines from chromosomes 1 to 22 and p and q are telomeres.

Table 2. Comparison of copy number aberrations between metastatic primary tumors and lymph node metastases

Chromosomal band	Chromosomal region (bp)		MPT n=15	LNM n=15	Fisher's exact test *p*-value
	Start	Stop			
*(Gains)**					
3q					
3q22.3	137531759	137722921	6	8	0.715
3q22.3	137934025	138196491	7	8	1
3q22.3-23-24	138273677	145205323	8	9	1
3q24	145547729	145646153	8	10	0.71
3q24	145827074	146012579	7	10	0.426
3q24-25.32	146407956	158853594	7	9	0.715
3q25.32-26.2	159199272	169830144	8	9	1
3q26.2-26.33	170039319	181002066	9	10	1
3q26.33	181075904	181236671	10	10	1
3q26.33-29	181381974	197282563	10	9	1
3q29	197289125	199251188	10	8	0.71
7p					
7p22.3	797378	1419664	5	8	0.462
7p22.3	1456404	2060814	5	9	0.272
7p22.2	2167170	3093625	5	10	0.143
7p22.2-13	3330242	43716929	5	9	0.272
7p13-12.2	43765914	50068258	5	10	0.143
7p12.2	50208728	50208787	4	9	0.139
7p12.2-12.1	50422509	53572980	4	10	0.066
7p12.1-11.2	53762968	56115221	5	10	0.143
7p11.2	56125603	56137483	5	9	0.272
8q					
8q11.1	47655222	47655281	10	11	1
8q11.1-11.21	48067862	48812138	10	12	0.682
8q11.21	48848611	48848670	10	13	0.39
8q11.21-13.3	48903308	73839888	11	13	0.651
8q13.3-22.1	73889304	94329172	12	13	1
8q22.1-24.3	94619246	142210616	12	14	0.6
8q24.3	142211510	142232729	13	14	1
8q24.3	142274933	144840107	13	15	0.483
8q24.3	144871892	145985998	12	14	0.6
8q24.3	145986495	145986541	12	13	1
8q24.3	146024157	146024209	12	12	1
8q24.3	146031718	146201771	11	12	1
8q24.3	146250765	146250824	11	11	1
9p					
9q22.2-32	91024411	115039890	8	7	1
9q32-33.2	115063679	125762928	9	8	1
9q33.3-34.11	125820201	129424744	10	8	0.71
9q34.11	129453688	129453747	10	9	1
9q34.11	129482231	129482290	10	10	1
9q34.11-34.13	129531368	134397227	11	11	1
9q34.13-34.3	134451067	139827325	11	12	1

number aberrations across the entire genome; however, between metastatic primary tumors and paired lymph node metastases genomic profiles have also shown some distinctive differences (data not shown). Additionally, we found the similarity in the genomic profile of the lymph node metastases and the paired metastatic primary tumor for the 15 clustered pairs as unsupervised hierarchical clustering data from metastatic primary tumors and lymph node metastases grouped together 15 out of the 18 pairs. Furthermore, by calculating the concordance rates significant similarities were analyzed between metastatic primary tumors and paired or non-paired lymph node metastases (on the basis of "Materials and Methods" section). The metastatic primary tumor and the paired lymph node metastases in 16 of the 18 cases had highest concordance rate (data not shown). We saw that the median of the concordance rate ($P< 0.01$; as per Mann Whitney U test) for non-paired samples had lower values than those for paired samples. Thus our results suggested that metastatic primary tumors and paired lymph node metastases contain predominantly clonal tumor cells. Besides, there was probable existence of minor subpopulations with different copy number aberrations in metastatic OSCCs.

Furthermore, we compared the number of copy number aberrations between metastatic primary tumors and paired lymph node metastases, in order to find out pos-

9q34.3	139853305	139853364	11	11	1
9q34.3	139879714	140128736	9	10	1
11q					
11q13.1	65684222	66143030	6	8	0.715
11q13.1-13.2	66153613	67157063	7	8	1
11q13.2	68061824	68943607	8	8	1
11q13.2-13.3	69131640	69954969	9	9	1
11q13.3	70012764	70182767	8	8	1
14q					
14q11.2	22307429	22689689	6	9	0.466
14q11.2	22722071	22846652	7	9	0.715
14q11.2-12	22863786	23720127	8	9	1
14q12	23728455	23809579	7	9	0.715
14q12	23837514	23837573	7	8	1
14q24.3	75940775	76019722	8	6	0.715
14q32.32-32.33	102408026	104704559	7	8	1
14q32.33	104763486	105067594	6	8	0.715
16p					
16p13.3	568884	3081611	5	8	0.46
17q					
17q24.3	67021962	67198033	5	8	0.462
17q24.3	67580412	67633808	5	9	0.272
17q24.3-25.1	67761999	69952626	6	9	0.466
17q25.1	69982273	70367509	6	10	0.272
17q25.1-25.3	70376047	73728901	7	11	0.264
17q25.3	73791333	78154478	6	11	0.139
17q25.3	78189789	78218020	6	10	0.272
17q25.3	78238617	78478382	6	9	0.466
17q25.3	78491903	78562713	6	8	0.715
17q25.3	78586237	78586290	5	8	0.46
20q					
20q11.21	29436537	29436596	8	7	1
20q11.21	29440414	30258071	8	8	1
20q11.21	30263613	31448563	8	9	1
20q11.21-12	31473449	37107764	9	9	1
20q12	37196884	37781860	8	9	1
20q12	37914814	38341204	7	8	1
20q12-13.32	38491408	56685769	6	8	0.715
20q13.32-13.33	56687771	60188703	7	8	1
20q13.33	60205864	62202076	8	8	1
20q13.33	62213501	62343283	6	8	0.715
(Losses)#					
3p					
3p26.3	224727	224786	7	9	0.715
3p26.3	261300	490711	9	9	1
3p26.3	653211	653268	9	10	1
3p26.3	660481	902607	10	10	1
3p26.3-25.1	1084890	14691701	11	10	1
3p24.3	14731775	14780134	12	10	0.682

sibility of the requirement of acquisition of copy number aberrations tumor cells spreading from the primary site to regional lymph nodes. Out of total 18 cases, 9 cases showed an increase in the number of copy number aberrations in the lymph node metastases while decrease was shown in 7 cases and no effect was observed in remaining 2 cases (data not shown). Thus, no significant differences were observed in the values of number of copy number aberrations between metastatic primary tumors and paired lymph node metastases (P=0.689). Furthermore, the frequencies of copy number aberrations were compared between grouped samples of metastatic primary tumors and lymph node metastases (**Figure 5A**) in order to identify any correlation between copy number aberrations and lymph node metastasis. In spite of this, we couldn't find even a single copy number aberration that was significantly more common in lymph node metastases (**Table 2**). Thus we may say that there is no requirement of additional copy number aberrations in spreading of tumor cells from the primary site to regional lymph nodes in OSCC.

Metastasis association of copy number aberrations with OSCCs

As shown in **Figure 5A**, the frequencies of copy number aberrations were not significantly different with respect to metastatic primary tumors and paired lymph node metastases we hypothesized the presence of subpopula-

3p24.3	14808514	15439619	12	11	1
3p24.3-22.2	15446399	38000505	12	12	1
3p22.2-11.2	38013228	88360589	12	11	1
3p11.2	88386457	88386516	11	11	1
3p11.2-11.1	88510901	90264177	11	10	1
4q					
4q31.1	1.51E+08	151243172	8	3	0.128
4q32.1-35.2	1.56E+08	189257416	8	5	0.462
8p					
8p23.2-23.1	3253003	6770153	6	8	0.715
8p23.1-12	6780746	35334886	7	8	1
8p11.23	39128088	39295715	6	8	0.715
18q					
18q11.2-12.1	22126166	23784984	6	8	0.715
18q12.1	23819557	28364284	8	9	1
18q12.1	28467152	30544333	9	10	1
18q12.1-21.2	30652551	46444013	10	10	1
18q21.2	46480704	46578751	9	9	1
18q21.2-22.1	46605530	59851815	10	10	1
18q22.1-23	59916041	72201527	11	10	1
18q23	72268316	73110608	10	10	1
18q23	73140033	73758157	9	10	1
18q23	73938538	75745646	9	9	1

*Genomic gains or #genomic losses detected in more than 50% of metastatic primary tumors or lymph node metastases are listed; MPT: metastatic primary tumors; LNM: lymph node metastases.

tions carrying metastasis-related copy number aberrations in metastatic primary tumors along with in lymph node metastases. Besides, there was a possibility of presence of non-metastatic subpopulations in metastatic primary tumors. These were supported by **Figure 4B** showing case 10 in which 2p was lost in the metastatic primary tumor but not in the lymph node metastases. We compared genomic profiles of lymph node metastases of metastatic OSCC and those of non-metastatic primary tumors (data not shown) for investigating the involvement of specific copy number aberrations in cervical lymph node metastasis. We detect losses at 3, 8-10p, 4, 13, 18, 21q and gains at 3, 9, 14, 20q, 16, 18p, 11q13 at more than 50% frequency in both the aforementioned cases (**Figure 5B**). These results suggested the possible involvement of these copy number aberrations in the development of OSCC. While differential detection in gains at 7p and 8,17q were observed in lymph node metastases ($P<0.05$, **Figure 5B**) and indicated the possible involvement of these copy number aberrations in the lymph node metastasis of OSCC. Besides, there was another interesting result of less frequent losses at 1,9,19p and 5q in lymph node metastases than non-metastatic primary tumors which have suggested the possible relation of non-metastatic phenotype of OSCC cells with these copy number aberrations.

Discussion

We observed the most similar genomic profiles of metastatic primary tumors and paired lymph node metastases in 16 out of 18 cases of metastatic OSCC (data not shown). Besides 15 out of 18 metastatic primary tumor-lymph node metastases pairs were grouped through unsupervised hierarchical clustering. This result has suggested the sharing of a similar genomic profile pattern between that the metastatic primary tumor and paired lymph node metastases. We observed almost similar average frequency values frequencies of copy number aberrations in metastatic primary tumors and also in lymph node metastases cases (**Figure 5A**). In this study we also observed some distinctive genomic copy number aberration patterns between the metastatic primary tumor and paired lymph node metastases in all of the cases of metastatic OSCC (detailed data not shown). Meanwhile, we observed that in 14 of the 18 metastatic OSCCs copy number aberrations were found which were found only in the metastatic primary tumor but remained undetected in the lymph node metastases. This suggests the tumor cells in the paired lymph node metastases are not responsible for all copy number aberration values detected in the metastatic primary tumor. This was further supported by case 10 in which 2p was lost only in the metastatic primary tumor and remained untouched in the lymph node metastases cases (**Figure 4A**). Thus we may say that genetically distinct subpopulations co-exist in nature. Thus we may say through our results that genetically clonal tumor cells have composed the meta-

static primary tumor cells and paired lymph node metastases with the inclusion of possible admixing of small genetically heterogeneous subpopulations in metastatic OSCC. Thus, our hypothetical model (**Figure 1**) has been justified. Specifically, we could say that these metastasis subpopulations would be responsible to lymph node metastasis in order to yield a large section of the subsequent lymph node metastases. Genetically distinct subpopulations through clonal evolution might be developed by a few subpopulations in lymph node metastases. Hence we proposed this hypothesis by keeping an eye towards the future that the progression of OSCC will be verified by these sequencing methods.

Gains at 7p and 8,17q were more frequently detected in lymph node metastases rather than in non-metastatic primary tumors, in this study, which is suggesting an association of copy number aberrations with former ones. Involvement of gain at 7p in lymph node metastasis of OSCC has already been reported [34, 35]. While 8q is frequently [26, 36] showing gain in OSCCs but relation of it with node metastasis of OSCC were not explored till now. Besides, till now, a little is known about the gain of 17q which was anticipated as a new member copy number aberration with respect to OSCC's lymph node metastasis, in the present study. However, association of lymph node metastasis with copy number aberrations was previously explored: gain at 7p, 11q13 and 20q along with loss at 8p were identified so far [28, 34, 35, 37]. In repeated studies (>3), we identified gains at 7p and 11q13 with respect to copy number aberrations of lymph node metastasis which concludes the importance of the role of copy number aberrations in the metastasis of OSCC. We also identified 7p's gain with respect to copy number aberrations of lymph node metastasis, but that was not with 11q13's gain. A plausible explanation, for this, could be that we have chosen tumors having tumor thickness of >4 mm while other groups selected non-metastatic OSCC samples randomly. High frequencies (55-91%) of metastatic OSCCs with gains at 7p, 8 or 17q in both the aforementioned cases were observed in this study. Based on these results, we may say that gains at these copy number aberrations might lead to the risk of high lymph node metastasis highly in the patients of primary tumor. This is very important suggestion for the diagnosis and treatment of OSCC as so far primary tumor is the deciding factor in the majority of current therapeutic strategies.

Figure 5B showed the losses at 3, 8-10p, 4, 13, 18, 21q and gains at 3, 9, 14, 20q, 16, 18p, 11q13 at a high frequency in both the studied cases. The frequency values of copy number aberrations were compared in present study with earlier less important report [38], so that we may determine the generalization of this tendency in OSCC analysis (detailed data not shown). Most copy number aberrations have shown relatively lower frequency (with exceptions in the frequency of 8q and 17q gain) in comparison to our analysis. At this time we can't explain this irregular behavior due to shortage of information with respect to lymph node status in the data.

In conclusion, we achieved that primary tumors of OSCC and their corresponding lymph node metastases share very similar patterns in terms of genomic copy number aberrations. Besides, a tendency of conversion of cells in the primary tumor into metastatic form was observed just after acquiring the copy number aberrations with respect to metastasis during clonal evolution, for example, gains at 7p and 8, 17q. Our work will be helpful in the prediction and treatment of lymph node metastases through the determination of metastasis-associated in biopsy samples from patients with OSCC. At this present time we may suggest to explore our work, in future, to clarify the mechanisms revealing the process of lymph node metastasis.

Disclosure of conflict of interest

None.

Address correspondence to: Bing Wen, Department of Stomatology, The First Affiliated Hospital of Nanchang University, 17 Yongwaizheng Avenue, Nanchang 330006, China. Tel: 0086-791-88696703; Fax: 0086-791-88696703; E-mail: wenbing493@hotmail.com

References

[1] Williams HK. Molecular pathogenesis of oral squamous carcinoma. Mol Pathol 2000; 53: 165-172.

[2] Jemal A, Siegel R, Ward E, Hao Y, Xu J and Thun MJ. Cancer statistics, 2009. CA Cancer J Clin 2009; 59: 225-249.

[3] Parkin DM, Laara E and Muir CS. Estimates of the worldwide frequency of sixteen major cancers in 1980. Int J Cancer 1988; 41: 184-197.
[4] Matsuda T, Marugame T, Kamo KI, Katanoda K, Ajiki W and Sobue T. Cancer incidence and incidence rates in Japan in 2003: based on data from 13 population-based cancer registries in the monitoring of cancer incidence in Japan (MCIJ) project. Japanese J Clin Oncol 2009; 39: 850-858.
[5] Wreesmann VB, Wang D, Goberdhan A, Prasad M, Ngai I, Schnaser EA, Sacks PG and Singh B. Genetic abnormalities associated with nodal metastasis in head and neck cancer. Head Neck 2004; 26: 10-15.
[6] Kalnins IK, Leonard AG, Sako K, Razack MS and Shedd DP. Correlation between prognosis and degree of lymph node involvement in carcinoma of the oral cavity. Am J Surg 1977; 134: 450-454.
[7] Yu S, Li J, Li Z, Zhang W and Zhao J. Efficacy of supraomohyoid neck dissection in patients with oral squamous cell carcinoma and negative neck. Am J Surg 2006; 191: 94-99.
[8] Keski-Santti H, Atula T, Tornwall J, Koivunen P and Makitie A. Elective neck treatment versus observation in patients with T1/T2 N0 squamous cell carcinoma of oral tongue. Oral Oncol 2006; 42: 96-101.
[9] Clark JR, Naranjo N, Franklin JH, de Almeida J and Gullane PJ. Established prognostic variables in N0 oral carcinoma. Otolaryngol Head Neck Surg 2006; 135: 748-753.
[10] Layland MK, Sessions DG and Lenox J. The influence of lymph node metastasis in the treatment of squamous cell carcinoma of the oral cavity, oropharynx, larynx, and hypopharynx: N0 versus N+. Laryngoscope 2006; 115: 629-639.
[11] Dias FL, Lima RA, Kligerman J, Farias TP, Soares JR, Manfro G and Sa GM. Relevance of skip metastases for squamous cell carcinoma of the oral tongue and the floor of the mouth. Otolaryngol Head Neck Surg 2006; 134: 460-465.
[12] Capote A, Escorial V, Munoz-Guerra MF, Rodríguez-Campo FJ, Gamallo C and Naval L. Elective neck dissection in early-stage oral squamous cell carcinoma- does it influence recurrence and survival? Head Neck 2007; 29: 3-11.
[13] P Oc, Pillai G, Patel S, Fisher C, Archer D, Eccles S and Rhys-Evans P. Tumor thickness predicts cervical nodal metastases and survival in early oral tongue cancer. Oral Oncol 2003; 39: 386-390.
[14] Asakage T, Yokose T, Mukai K, Tsugane S, Tsubono Y, Asai M and Ebihara S. Tumor thickness predicts cervical metastasis in patients with stage I/II carcinoma of the tongue. Cancer 1998; 82: 1443-1448.
[15] Pentenero M, Gandolfo S and Carrozzo M. Importance of tumor thickness and depth of invasion in nodal involvement and prognosis of oral squamous cell carcinoma: a review of the literature. Head Neck 2005; 27: 1080-1091.
[16] Huang SH, Hwang D, Lockwood G, Goldstein DP and O'Sullivan B. Predictive value of tumor thickness for cervical lymph-node involvement in squamous cell carcinoma of the oral cavity: a meta-analysis of reported studies. Cancer 2009; 115: 1489-1497.
[17] Xu C, Liu Y, Wang P, Fan W, Rue TC, Upton MP, Houck JR, Lohavanichbutr P, Doody DR, Futran ND, Zhao LP, Schwartz SM, Chen C and Méndez E. Integrative analysis of DNA copy number and gene expression in metastatic oral squamous cell carcinoma identifies genes associated with poor survival. Mol Cancer 2010; 9: 143.
[18] Vogelstein B and Kinzler KW. Cancer genes and the pathways they control. Nat Med 2005; 10: 789-799.
[19] Merlo LM, Pepper JW, Reid BJ and Maley CC. Cancer as an evolutionary and ecological process. Nat Rev Cancer 2006; 6: 924-935.
[20] Polyak K. Is breast tumor progression really linear? Clin Cancer Res 2008; 14: 339-341.
[21] Heng HH, Stevens JB, Bremer SW, Ye KJ, Liu G and Ye CJ. The evolutionary mechanism of cancer. J Cell Biochem 2010; 109: 1072-1084.
[22] Weigelt B, Peterse JL and van't Veer LJ. Breast cancer metastasis: markers and models. Nat Rev Cancer 2005; 5: 591-602.
[23] Bernards R and Weinberg RA. A progression puzzle. Nature 2002; 418: 823.
[24] Pollack JR, Perou CM, Alizadeh AA, Eisen MB, Pergamenschikov A, Williams CF, Jeffrey SS, Botstein D and Brown PO. Genome-wide analysis of DNA copy-number changes using cDNA microarrays. Nat Genet 1999; 23: 41-46.
[25] Davies JJ, Wilson IM and Lam WL. Array CGH technologies and their applications to cancer genomes. Chromosome Res 2005; 13: 237-248.
[26] Garnis C, Coe BP, Zhang L, Rosin MP and Lam WL. Over-expression of LRP12, a gene contained within an 8q22 amplicon identified by high-resolution array CGH analysis of oral squamous cell carcinomas. Oncogene 2005; 23: 2582-2586.
[27] Chung CH, Parker JS, Karaca G, Wu J, Funkhouser WK, Moore D, Butterfoss D, Xiang D, Zanation A, Yin X, Shockley WW, Weissler MC, Dressler LG, Shores CG, Yarbrough WG and Perou CM. Molecular classification of head and neck squamous cell carcinomas using patterns of gene expression. Cancer Cell 2004; 5: 489-500.

[28] Liu CJ, Lin SC, Chen YJ, Chang KM and Chang KW. Array-comparative genomic hybridization to detect genome wide changes in microdissected primary and metastatic oral squamous cell carcinomas. Mol Carcinog 2006; 45: 721-731.

[29] Freier K, Knoepfle K, Flechtenmacher C, Pungs S, Devens F, Toedt G, Hofele C, Joos S, Lichter P and Radlwimmer B. Recurrent copy number gain of transcription factor SOX2 and corresponding high protein expression in oral squamous cell carcinoma. Genes Chromosomes Cancer 2010; 49: 9-16.

[30] Noutomi Y, Oga A, Uchida K, Okafuji M, Ita M, Kawauchi S, Furuya T, Ueyama Y and Sasaki K. Comparative genomic hybridization reveals genetic progression of oral squamous cell carcinoma from dysplasia via two different tumourigenic pathways. J Pathol 2006; 210: 67-74.

[31] Patmore HS, Ashman JN, Cawkwell L, MacDonald A, Stafford ND and Greenman J. Can a genetic signature for metastatic head and neck squamous cell carcinoma be characterised by comparative genomic hybridisation? Br J Cancer 2004; 90: 1976-1982.

[32] Bockmuhl U, Schluns K, Schmidt S, Matthias S and Petersen I. Chromosomal alterations during metastasis formation of head and neck squamous cell carcinoma. Genes Chromosomes Cancer 2002; 33: 29-35.

[33] Navin N, Kendall J, Troge J, Andrews P, Rodgers L, McIndoo J, Cook K, Stepansky A, Levy D, Esposito D, Muthuswamy L, Krasnitz A, McCombie WR, Hicks J and Wigler M. Tumour evolution inferred by single-cell sequencing. Nature 2010; 472: 90-94.

[34] Chen YJ, Lin SC, Kao T, Chang CS, Hong PS, Shieh TM and Chang KW. Genome-wide profiling of oral squamous cell carcinoma. J Pathol 2006; 204: 326-332.

[35] Pathare SM, Gerstung M, Beerenwinkel N, Schäffer AA, Kannan S, Pai P, Pathak KA, Borges AM and Mahimkar MB. Clinicopathological and prognostic implications of genetic alterations in oral cancers. Oncol Lett 2011; 2: 445-451.

[36] Garnis C, Coe BP, Ishkanian A, Zhang AL, Rosin MP and Lam WL. Novel regions of amplification on 8q distinct from the MYC locus and frequently altered in oral dysplasia and cancer. Genes Chromosomes Cancer 2006; 39: 93-98.

[37] Sugahara K, Michikawa Y, Ishikawa K, Shoji Y, Iwakawa M, Shibahara T and Imai T. Combination effects of distinct cores in 11q13 amplification region on cervical lymph node metastasis of oral squamous cell carcinoma. Int J Oncol 2011; 39: 761-769.

[38] Cai H, Kumar N and Baudis M. arrayMap: a reference resource for genomic copy number imbalances in human malignancies. PLoS One 2012; 7: e36944.